Scientific paper

Selective Removal of Sodium Ions from Aqueous Media Using Effective Adsorbents: Optimization by RSM and Genetic Algorithm

Lei Yao,[1,*] Chao Hong,[2] Hani Dashtifard[3] and Hossein Esmaeili[4]

[1] *College of Civil and Architecture Engineering, Chuzhou University, Chuzhou 239000, Anhui, China*

[2] *Nanjing Siweipu Environmental Protection Technology Co., Ltd., Nanjing 210000, Jiangsu, China*

[3] *Department of Chemical Engineering, Bushehr Branch, Islamic Azad University, Bushehr, Iran*

** Corresponding author: E-mail: yaolei@chzu.edu.cn*

Received: 02-19-2021

Abstract

This study aimed to determine the best adsorbent among *Moringa oleifera*-derived activated carbon (AC), eggshell-derived CaO nanoparticles and CaO/Fe_3O_4 for sodium (Na^+) removal from aqueous media. In the first step, the appropriate adsorbent for sodium adsorption was determined among the three adsorbents, which the results showed that the AC had the highest sorption efficiency. Then, response surface methodology (RSM) was used to evaluate the impact of different factors on the Na^+ ion sorption efficiency using the AC. The highest removal efficiency was obtained to be 95.91% at optimum conditions such as pH of 11, contact time of 45 min, temperature of 25 °C, sodium ion concentration of 900 mg/L, and adsorbent dosage of 5 g/L. Also, the best conditions using the genetic algorithm was obtained at contact time of 94.97 min, adsorbent dosage of 3.52 g/L, Na^+ ion concentration of 939.92 mg/L and pH value of 10.92. Moreover, the maximum sorption capacity using the Langmuir model was obtained to be 249.67 mg/g, which was a significant value. Besides, the equilibrium and kinetic studies indicated that the experimental data of sodium adsorption process were fitted well with the Langmuir isotherm model and the pseudo-second-order kinetic model, respectively. Furthermore, the thermodynamic study indicated that the sorption process was endothermic. Generally, among the three adsorbents used, activated carbon with a high removal efficiency and significant sorption capacity can be considered as a promising adsorbent for the removal of sodium from wastewater on an industrial scale.

Keywords: Adsorption, sodium, *Moringa oleifera*, Response surface methodology (RSM), Genetic algorithm

1. Introduction

For the past several decades, there has been a growing concern about water pollution, which affects animals, plants, and humans.[1,2] Sea water is a good source of sodium ion, the salinity which does not allow humans to consume it. Sodium ion is a major component in the sea water, where its weight percent is about 16 times higher than magnesium ions, about 22 times higher than sulfur ions and about 48 times higher than bromine and potassium ions.[3] The shortage of water resources and the risk of water crisis in the world as well as the pollution of surface and underground water resources with sodium ion and other pollutants from industrial and municipal sewage has made it necessary to find environmentally acceptable solutions for the elimination of these contaminants from water.[4] The main sources of water pollution with sodium are human activities. Excessive consumption of sodium over the standard level causes various sicknesses like high blood pressure, the risk of cardiovascular illnesses, heart attack, and damages to kidneys.[5]

There are various methods to eliminate pollutants from wastewater, including ion exchange, reverse osmosis, biological process, electrodialysis, distillation, and chemical precipitation.[6] The reverse osmosis and ion exchange processes can't selectively eliminate sodium ion and require continuous regeneration; these two processes do not make any chemical changes in sodium and result in pollut-

ed wastewater.[7,8] The biological process is mainly applied to wastewater and is not preferred for water treatment processes due to the application of organic materials and the need for maintenance. Furthermore, the resultant biological sludge needs to be treated before disposal.[9]

Adsorption process is more effective than other techniques in the elimination of pollutants, even at low concentrations (1 mg/L).[10] Depending on the type of the adsorbent, this simple and applicable method is superior from the aspects of capital cost, reuse of wastewater, simplicity, and flexibility of design, easy operation, and insensitivity to toxic compounds and pollutants.[11,12]

One of the main adsorbents used in this field is activated carbon (AC), which is made from various herbal resources. Activated carbon can be used to remove metal ions from water and wastewater due to many advantages such as the simplicity in its synthesis, high specific surface area, high sorption performance, low-cost, and ability to remove low concentrations of heavy metal ions.[13–15]

Iron oxide nanoparticles are also known to be an available, cheap, and environmentally friendly material for effective sorption of pollutants due to their easy synthesis process. The magnetic nature of these nanoparticles allows their easy separation from pollutants through an external magnetic field. Considering some properties like the area to volume ratio, easy separation, recovery of nanoparticles by using an external magnetic field, low toxicity, and possibility of surface modification of nanoparticle resulted in their high efficiency of sorption. Also, the surface of magnetic materials can be modified by other materials such as CaO to increase their adsorption capacity.[16–18]

Moreover, the eggshell is an important adsorbent for the elimination of dyes and heavy metals from wastewater and has been applied several times in previous studies.[19]

Different adsorbents have been used so far for removal of sodium ions from aqueous solutions, which some of them are included zeolites,[4] chitosan,[20] activated carbon made from rice husk[21] and polyantimonic acid.[22]

This study aims to compare the ability of cheap adsorbents like AC made from *Moringa oleifera* leaf, eggshell-derived CaO nanoparticles, and CaO/Fe_3O_4 composite in the removal of sodium ion from synthetic wastewater, which these adsorbents have not been used to remove sodium ions in previous studies. Different analyses such as X-ray diffraction (XRD), scanning electron microscope (SEM), Brunauer–Emmett–Teller (BET), and Fourier-transform infrared spectroscopy (FTIR) were used to determine the surface properties of the activated carbon. Also, different parameters such as temperature, contact time, pH, and sorbent dosage were studied on the Na^+ ion removal, and the best conditions were obtained using the response surface method (RSM). Also, the equilibrium, kinetic, and thermodynamic behaviors of the sorption process were studied. Moreover, genetic algorithm method was applied to optimize the best conditions for Na^+ removal using the AC, which is another innovation of this research.

2. Materials and Methods

2. 1. Chemicals

In this work, $FeCl_2.4H_2O$ and $FeCl_3.6H_2O$ were purchased from Merck Co. (Germany, purity>99%) and were used for preparing iron oxide. Sodium chloride (NaCl, purity>99%), sodium hydroxide (NaOH, purity>99%) and hydrochloric acid (HCl, purity=37%) were all supplied from Merck Co. (Germany). For the preparation of stock solution with 1000 ppm concentration, 2.543 g NaCl was dissolved in 1000 ml double distilled water. For preparing other solutions with lower concentrations, the stock solution was diluted with double distilled water.

2. 2. Preparation of Activated Carbon from Moringa Oleifera Plant

The *Moringa oleifera* is a native plant of Bushehr province (Iran), which was utilized to produce AC. To do this, the *Moringa oleifera* leaves were placed in a furnace at 650 °C for 4 hours and then was pulverized and sieved by a 25-mesh size sieve. Then, the resultant powder was kept in glass bottles for uptake tests. To determine surface characteristics of the AC, XRD, SEM, BET, and FTIR analyses were carried out. The XRD analysis was used to determine the crystalline phases of the AC. Additionally, SEM and FTIR analyses were done to determine the morphology and functional groups in the AC structure, respectively. Also, BET analysis was applied to determine the specific surface area of the adsorbent.

2. 3. Preparation of CaO and CaO/Fe_3O_4 from Eggshell Waste

To prepare CaO, eggshell wastes were first washed for several times with tap water and then was placed in an oven at 105 °C to be dried completely. After being dried, the eggshells were placed in a furnace at 800 °C for 4 hours. After this time, the eggshells were cooled down at room temperature. The calcined eggshells were pulverized in a mill and then stored in plastic bottles.[13] To support Fe_3O_4 nanoparticles on the CaO structure obtained from eggshells, a solution containing Fe^{+3} and Fe^{+2} with a 2:1 molar ratio was prepared. Then, about 1 g of CaO was added to the solution and it was blended for 20 min with mixing rate of 400 rpm. Then, sodium hydroxide with 3 M concentration was added dropwise to this solution, and the oxidation process progressed. The addition of sodium hydroxide was continued until a black colored solution was obtained. Afterwards, the prepared adsorbent was separated from the solution and washed with distilled water several times to be neutralized. After that, the adsorbent was placed in an oven at 105 °C for 24 hours to be completely dried. The dried adsorbent was then pulverized to be used in the uptake of sodium ion.

2. 4. Adsorption Test

The experiments were performed in a 200 ml Erlenmeyer, which were filled with 100 ml of sodium solution. Then, the impact of various factors like sodium concentration (300–1500 ppm), contact time (15–75 min), pH (3–11) and sorbent dosage (1–9 g/l) were studied on the Na^+ ion removal, and the best operating conditions for the removal of Na^+ ion were determined using Design Expert 10 and Central Composite Design (CCD) method.

Then, the solution was filtered using a fiber glass filter for elimination of solid particles. The filtered solution was analyzed to determine the residual Na^+. The pH of each sample was adjusted by hydrochloric acid (0.1 M) and sodium hydroxide (0.1 M). A flame atomic absorption spectroscopy (model Varian AA240, Australia) was applied to specify the residual Na^+ ion in the samples. In all samples, the Na^+ ion sorption percentage (R%) and sorption capacity (q) were determined using equations 1 and 2, respectively.

$$R\,(\%) = \frac{C_O - C_e}{C_o} \times 100 \quad (1)$$

$$q = (C_0 - C_e) \times \frac{V}{M} \quad (2)$$

where, C_o is the initial sodium concentration and C_e is the equilibrium sodium concentration after uptake process, R is the removal efficiency of Na^+, M is the weight of adsorbent in the solution (g) and V is the volume of the solution (L).

3. Results and discussion

3. 1. Determination of the Primary Efficiency of the Three Utilized Adsorbents

To evaluate the initial performance of the adsorbents, their adsorption efficiency in the removal of sodium ions was studied. To this end, experiments were performed at different contact times. Other conditions were kept constant, including pH of 7, temperature of 25 °C, Na^+ ion concentration of 900 mg/L, and adsorbent dosage of 5 g/L. Since these conditions have been used in most previous work to perform the sodium adsorption process, the adsorption experiments were performed under these conditions to compare the three adsorbents. Figure 1 indicates the sodium uptake efficiency from aqueous solution using the eggshell derived CaO, CaO/Fe_3O_4 composite, and AC prepared by *Moringa oleifera* plant leaves. As can be seen, the AC with an uptake efficiency of 79% has the maximum uptake efficiency compared to the other two adsorbents. According to Figure 1, the removal efficiency of Na+ using AC is about 25% higher than CaO/Fe_3O_4 and 35% higher than eggshell derived CaO and this difference in efficiency is observed at all times. Therefore, the AC was used for further experiments and to determine the optimal conditions for Na^+ ion removal.

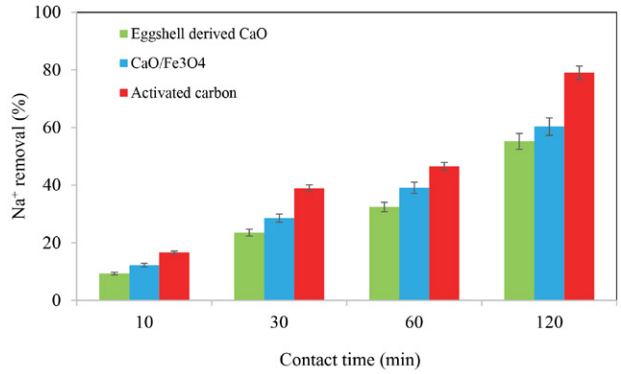

Figure 1. Primary investigations about three studied adsorbents in 10, 30, 60, and 120 min and neutral pH

3. 2. Characteristics of the Adsorbent

FTIR analysis was used to determine functional groups in the structure of *Moringa oleifera* leaves-derived AC as shown in Figure 2-a. These spectra approve the presence of many functional groups and indicate the natural complex of this material. As shown, the absorption peak at 3048 cm^{-1} is related to the tensile vibration of OH group in proteins, fatty acids, carbohydrates, and lignin, which are due to its high contents in plant grain as well as N-H tensile bonding in amides.[24–25] Also, the peak at 2895 cm^{-1} is related to the =C-H bond.[23] Moreover, the peaks at 795 cm^{-1} and 926 cm^{-1} are attributed to the N-H and O-H functional groups, respectively. Furthermore, the peaks at 1232.8, 1396.8, 1506 and 1615.6 cm^{-1} can be attributed to the C-O, C-H, C=C, and C=O, respectively.[24,26–28]

Also, SEM analysis was applied to characterize the morphology of the *Moringa oleifera*-derived AC and its image is seen in Figure 2-b. It is obvious that the AC has a relatively porous structure with heterogeneous distribution. Also, some pores are observed on the surface of the adsorbent that include the accessible sites. These pores provide suitable conditions for the uptake of Na^+ ions from aqueous solution.[29]

Moreover, XRD analysis is used to identify and evaluate the crystalline phases in the adsorbent structure. Generally, materials are classified into different groups of amorphous, semi-crystalline, and crystalline. Figure 2-c shows the XRD pattern of the AC. According to Figure 2-c, the adsorbent shows a long peak at $2\boldsymbol{\theta} = 20°$, which is attributed to the crystalline phase of (111) in the AC structure.[30,31]

Besides, BET analysis showed that the specific surface area, pore volume and mean pore diameter of the activated carbon prepared from *Moringa oleifera* leaves were obtained as 136.25 m^2/g, 0.158 cm^3/g, and 55 °A, respectively, which shows that the adsorbent has a significant specific surface area. Also, the mean pore size of the adsorbent indicates that the adsorbent has a mesoporous structure, because the mean pore size is between 2–50 nm.[13]

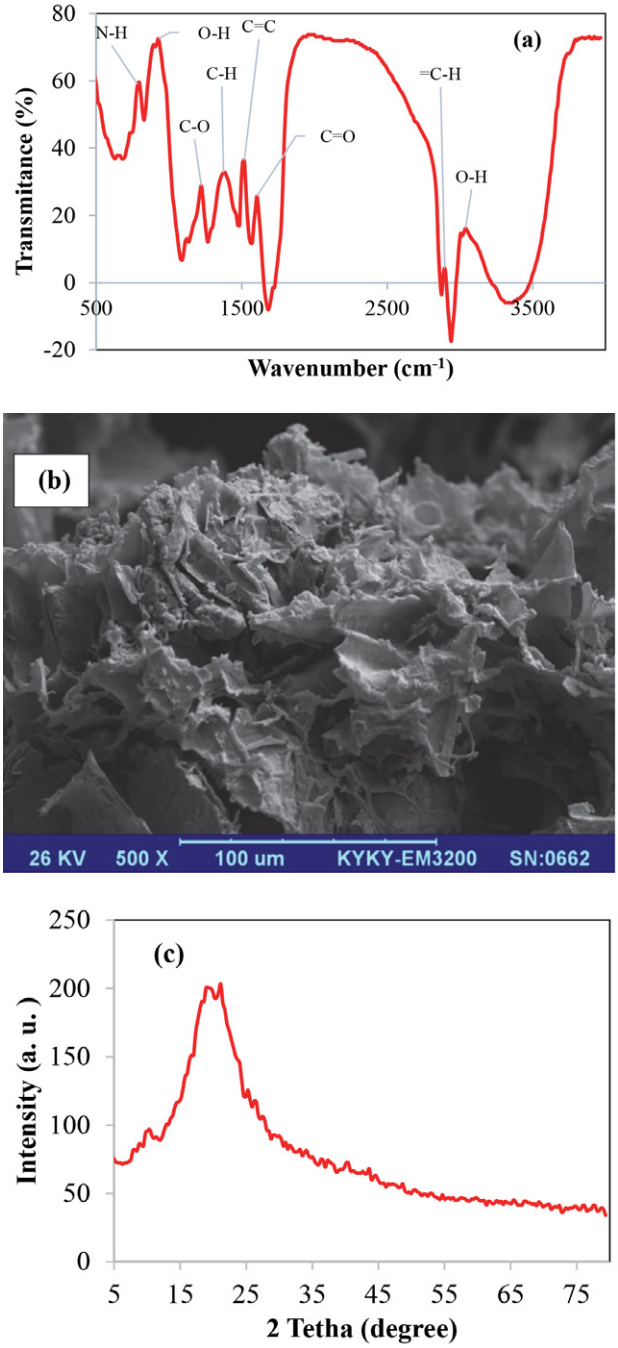

Figure 2. The characteristics of the activated carbon made from *Moringa oleifera* plant using various analyses, including FTIR (a), SEM (b), and XRD (c).

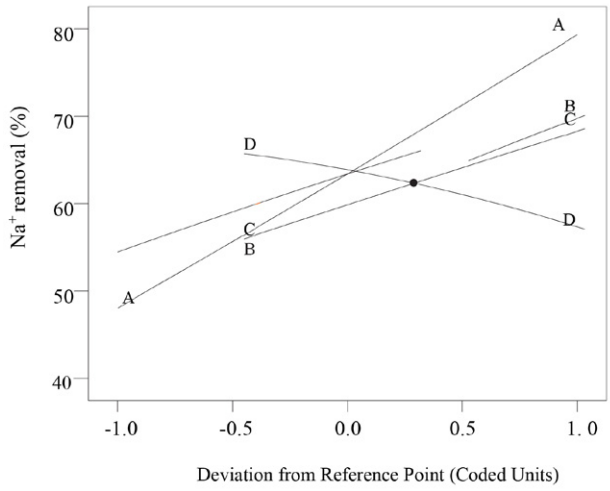

Figure 3. Effective parameters on adsorption process (separately and without any effect on each other) at pH of 7, contact time of 45 min, the adsorbent dosage of 5 g/L, and initial Na^+ concentration of 900 mg/l.

3. 3. Effective Parameters on the Sorption Process

The impact of various factors on the sodium ion sorption using the AC is demonstrated in Figure 3. As seen in this Figure, the uptake efficiency of Na^+ ion increases with increasing pH, contact time, and adsorbent dosage.

The impact of pH and Na+ concentration on the Na^+ ion removal efficiency using the AC simultaneously is shown in Figure 4. Other experimental conditions were kept constant, including contact time of 45 min, temperature of 25 °C, and adsorbent dosage of 5 g/L. According to the results, the sorption efficiency increased with increasing the pH value from 3 to 11 and the maximum sorption efficiency was obtained at pH = 11. The formation of hydroxide ion (OH^-) and its bonding to the surface of the adsorbent makes the adsorbent surface negatively charged and the adsorbent ability increases in the sorption of cations. The reason of reduction in the adsorption efficiency in acidic pH might be that the increase in hydrogen ion production creates a positive charge on the adsorbent surface (protonation of the adsorbent).[32] In other words, the pH of zero point charge (isoelectric pH) plays an important role in the adsorption process. Since this pH was obtained about 6.5 for the studied adsorbent, the *Moringa oleifera* adsorbent surface will be negatively charged in higher pH values and consequently, a strong electrostatic attraction will form between the surface groups and available cations (Na^+). Therefore, the adsorption efficiency was increased and the maximum sodium ion adsorption efficiency was obtained 95.53%, but in pH values less than the isoelectric point, the adsorbent surface is positively charged and forms a stable electrostatic repulsion force, which reduces the sorption of Na^+ ions. Another reason for the reduction in Na^+ ion adsorption in acidic conditions is the strong competition between the hydrogen ion (H^+) and positively charged sodium ions to be adsorbed on the adsorbent surface, which decreases the adsorption efficiency.

Therefore, pH = 11 was selected as the optimum pH and further adsorption experiments were carried out at

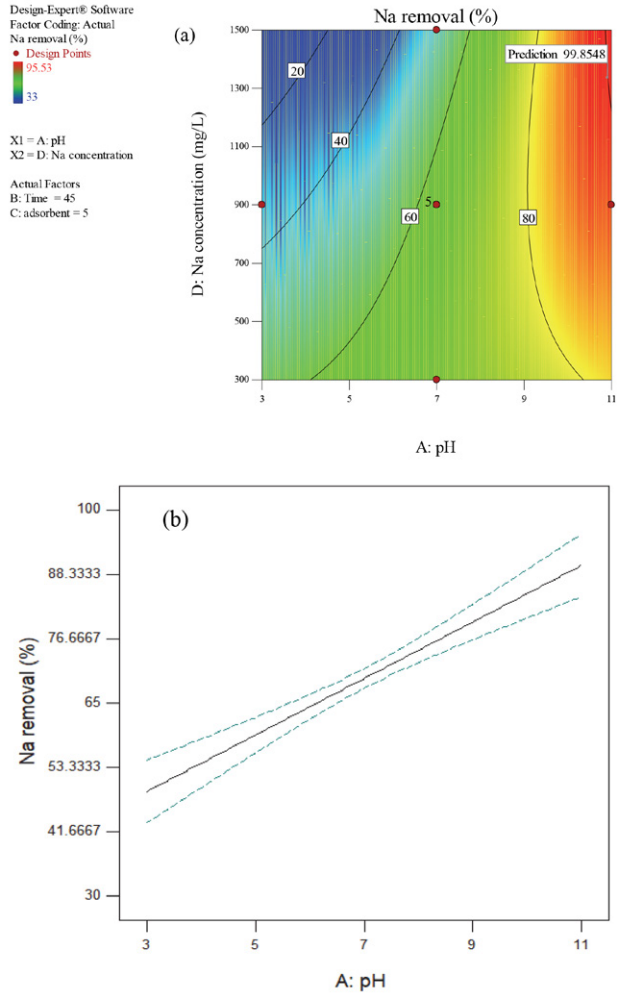

Figure 4. The effect of pH on the sodium ion adsorption from an aqueous solution using the AC in different concentrations of sodium ion

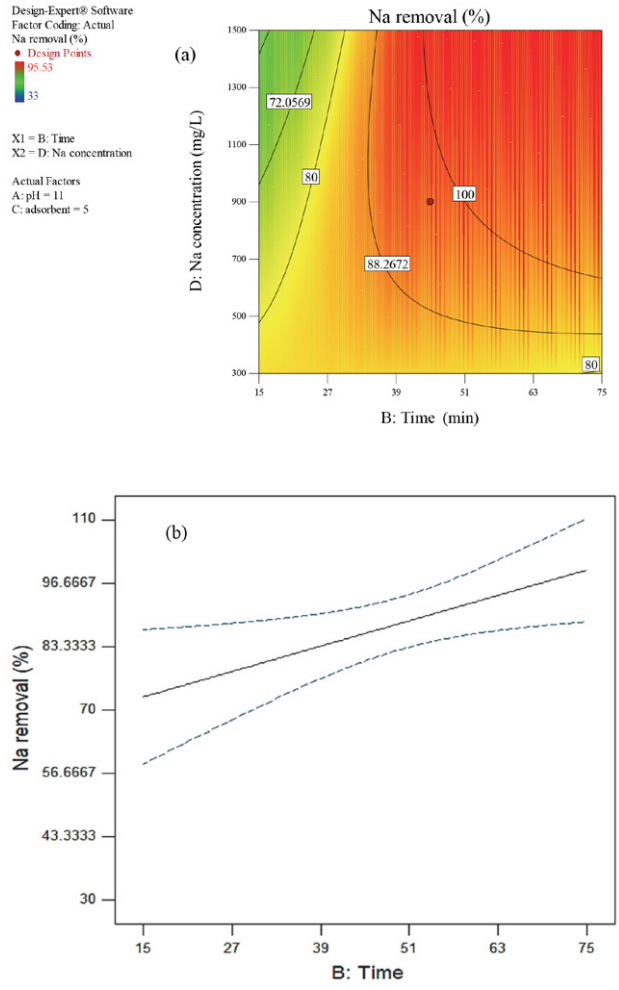

Figure 5. The effect of contact time on sodium adsorption from aqueous solution using the AC in different sodium ion concentrations

this pH value. Figure 5 shows the effect of contact time on the sorption efficiency of sodium using the activated carbon, in different sodium concentrations. Experiments were carried out at pH=11 (the optimum value) and adsorbent dosage of 3.5 g/L. As can be seen, increasing the contact time has increased sodium adsorption efficiency and then it has reached the equilibrium value. Changes in the adsorbent capacity, when contact time increases, indicated that in the first 45 min, the intensity of changes was high and then the adsorption trend became constant. Rapid enhancement of adsorption capacity in the early stages of the adsorption process was due to the high number of active sites for sodium adsorption on the adsorbent surface. When the process continued, the access of ions to the active sites was reduced, and eventually, the adsorption process reached an equilibrium at a specific time. After the equilibrium, there might be negligible changes in the adsorption capacity. Therefore, the optimum contact time was attained 47 min.

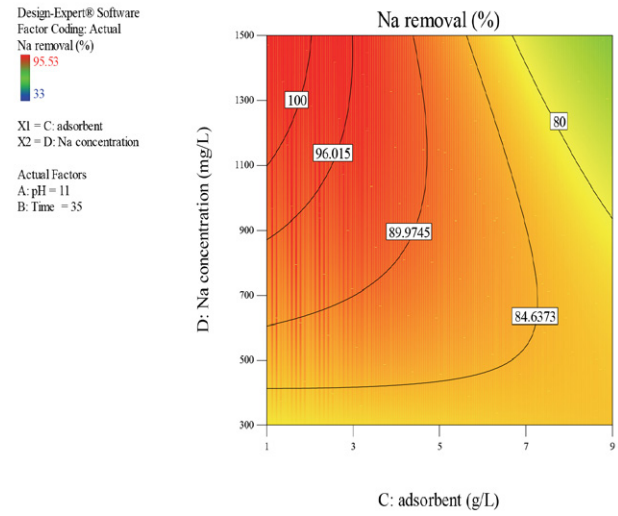

Figure 6. Effect of adsorbent dose on sodium adsorption from aqueous solutions in different concentrations of sodium ion

The effect of adsorbent dosage on sodium ion adsorption efficiency is indicated in Figure 6. According to the results, the removal efficiency increases with increasing adsorbent dosage, which is due to the enhancement of active sites on the adsorbent surface.[19] The research results indicated that the enhancement of the initial concentration of sodium ion decreases the adsorption efficiency, which is due to the saturation of the adsorbent surface in high sodium concentrations.

Nowadays, using statistical design and presenting logical correlations between variables is widely used in many research fields. Using statistical methods decreases the number of experiments and as a result, the costs and manpower.[33–34] Utilization of statistical method in this study resulted in the following equation that shows the empirical correlation between experimental variables and efficiency percentage in a coded form:

$$\begin{aligned} Na^{+}removal = {} & 63.4 + 15.63A + 8.47B \\ & + 6.51C - 4.47D + 0.95AB - 5.45AC \\ & + 4.65AD - 0.51BC + 5.47BD - 2.3C \\ & + 0.3A^2 - 0.46B^2 - 0.07C^2 \end{aligned} \quad (3)$$

X_1, X_2, X_3, and X_4 show the pH, contact time, adsorbent dosage, and pollutant concentration, respectively. The effect of studied parameters on the sorption efficiency of sodium ion was investigated by analysis of variance (ANOVA) and the outcomes are presented in Table 1.

The values of $R^2 = 0.9950$ and Adj $R^2 = 0.9834$ verifies that sodium adsorption by the activated carbon made from *Moringa oleifera* can be well explained by the designed model. Also, the F-value was obtained 85.88, which shows the ability of the selected model in data analysis. The low value of CV also verifies that this model is suitable for interpretation of the studied process. Adequate precision is the parameter that indicates the ratio of signal to noise; if its value is more than 4, it shows an appropriate relation between the experimental data and the calculated values (desirability). In this study, the mentioned parameter was obtained 38.36. Then, the influence of the effective parameters on the uptake process of Na^+ was studied using the analysis of variance. The results indicated that X_1, X_2, X_3, X_4, X_1X_3, X_1X_4, X_2X_4, and X_3X_4 parameters had significant effect ($P < 0.05$) on sodium adsorption.[34] The sequence of two parameters of the sum of squares and F-value was pollutant concentration< adsorbent dosage< contact time< pH that indicates the maximum effect of pH and the minimum effect of pollutant concentration on the Na^+ removal. Investigation of the normality of the studied data and the residuals, as two important assumptions, is essential for using this statistical model. The normal probability curve shows the normal distribution of data around a mean value and the linearity of this curve shows that experimental data are normal.

The R-squared value was obtained to be 0.942 from the normal probability curve. The test of normality of output data and residuals are shown in Figure 7.

Figure 7 shows the actual (experimental) and the predicted values of sodium adsorption by Design Expert 10 in 21 different runs. The high level of conformity of the actual value with the predicted one indicates the excellent ability of the software in the prediction of the experiment results in different runs.

Table 1. Results of the analysis of variance for the studied model

ANOVA for Response Surface Quadratic model					
Source	**Sum of Squares**	**df**	**Mean Square**	**F Value**	**p-value**
Model	4860.52	14	347.18	85.88	<0.0001
A-pH	1955.00	1	1955.00	483.57	<0.0001
B-Time	573.93	1	573.93	141.96	<0.0001
C-adsorbent	677.69	1	677.69	167.63	<0.0001
D-Na^+ concentration	159.85	1	159.85	0.90	<0.0008
AB	3.62	1	3.62	0.90	0.3806
AC	237.29	1	237.29	58.69	0.0003
AD	86.63	1	86.63	21.43	0.0036
BC	2.09	1	2.09	0.52	0.4991
BD	119.52	1	119.52	29.56	0.0016
CD	42.46	1	42.46	10.50	0.0177
A^2	2.47	1	2.47	0.61	0.4641
B^2	5.31	1	5.31	1.31	0.2954
C^2	0.13	1	0.13	0.032	0.8649
D^2	23.13	1	23.13	5.72	0.0539
Residual	24.26	6	4.04		
R^2	0.9950	R^2-Adjusted	0.9834	R^2-Predicted	0.9462

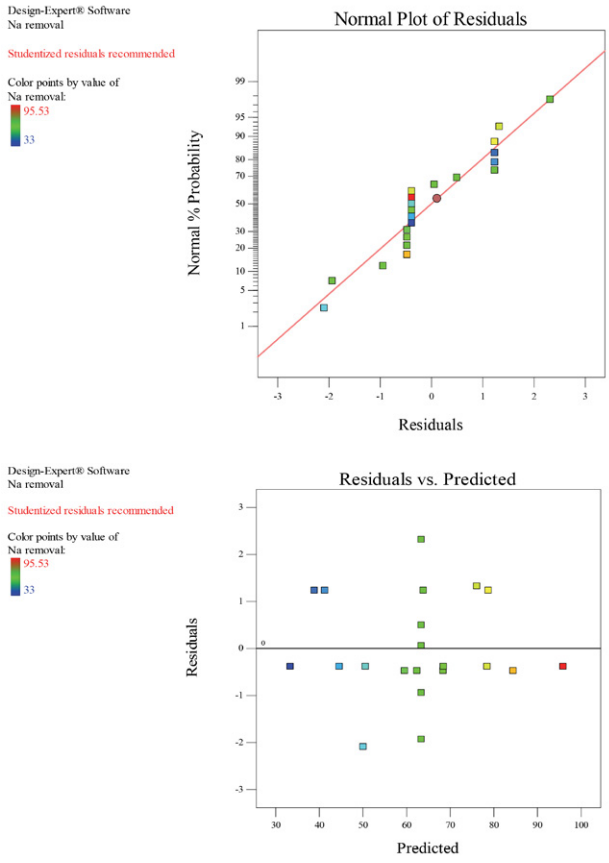

Figure 7. The normality of primary data and residuals

The very high value of R-square confirms the prediction ability of the Na^+ ion adsorption process in the studied system. Then, the real (experimental) values are plotted versus the predicted values and compared with each other. As predicted, the resulted R-square from regression was very close to 1.

3. 4. Prediction of Adsorption Process by the Software

In Table 2, independent variables and the range and levels of experimental values are presented for activated carbon as an adsorbent in the removal of Na^+ ions. In this study, the total number of experiments in the CCD design method was 21. Furthermore, the sorption efficiency of sodium ion in different experimental conditions was reported.

Figure 8(a) shows the actual and predicted values of sodium ion removal percentage using activated carbon in various experiments. The predicted values of sodium ion removal efficiency are extracted from Figure 8(a) and then reported in Table 2. As reported in Table 2, the maximum removal efficiency of N^+ ion was achieved 95.91%. Also, the value of R^2 coefficient was achieved 0.9975, which indicates a good ability of the model in the prediction of data.

Figure 8(b) also shows the experimental outcomes versus the predicted ones by Design Expert 10. As seen in this figure, the R^2 value of 0.9462 was achieved for the prediction, which verifies the results obtained in the previous stage.

Table 2. The impact of independent variables on the removal efficiency of sodium using AC. Experimental design was done by CCD method

Run	A: pH	B: Time (min)	C: adsorbent dose (g/L)	D: Na^+ conc. (mg/l)	Na^+ removal (%)	Predicted value of Na+ removal (%)
1	5	60	7	1200	59.11	59.58
2	11	45	5	900	95.53	95.91
3	7	45	9	900	77.45	76.12
4	5	60	3	1200	42.54	41.3
5	3	45	5	900	33	33.38
6	7	45	5	900	63.45	63.39
7	9	60	7	600	84	84.47
8	7	45	5	900	65.71	63.39
9	7	75	5	900	78.11	78.49
10	7	45	5	900	63.89	63.39
11	7	45	5	1500	50.23	50.61
12	9	30	7	1200	61.94	62.41
13	7	45	5	900	62.45	63.39
14	7	15	5	900	44.23	44.61
15	7	45	5	300	68.11	68.49
16	5	30	7	600	67.95	68.42
17	5	30	3	600	40.12	38.88
18	9	30	3	1200	65.11	63.87
19	7	45	5	900	61.46	63.39
20	9	60	3	600	80	78.76
21	7	45	1	900	48	50.09

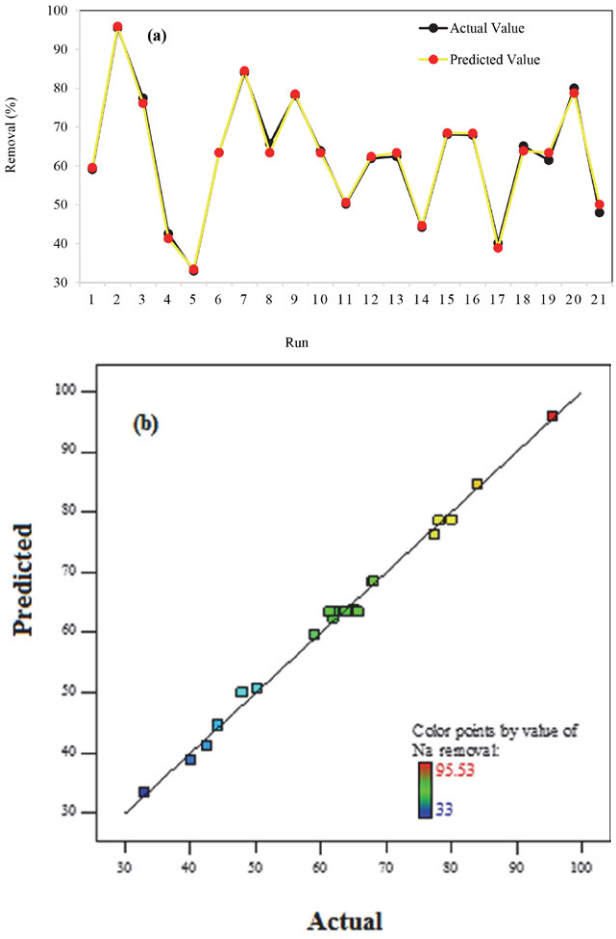

Figure 8. Predicted and real values of efficiency in different runs of the experiment (a) the experimental results versus the predicted results by the software (b)

3. 5. Optimization of Sodium Adsorption Process

Optimization of process conditions is necessary for any statistical model. To do this, Genetic Algorithm (GA) was applied for the optimization of Na^+ uptake process. In this model, the best conditions for eliminating Na^+ ions were determined. To optimize the uptake process, the studied parameters were selected in the range of their maximum and minimum values. In fact, the algorithm genetic method is capable of interpolating data and can optimize results. Therefore, interpolation between data is a prominent feature of the genetic algorithm method compared to the CCD method. The target variable (Na^+ removal efficiency (%)) was considered in the maximum value. The purpose of using the GA method was to determine the best conditions of the Na^+ removal and uses the results of the CCD method. After determining the optimal conditions by the CCD method, the data were entered into the software to optimize the parameters and to do this, Na^+ removal efficiency was considered as the response (target function).[35] It should be noted that before optimizing the effective parameters in the adsorption process, the studied algorithm has determined some points (Generation) in the first step, and then, in the next step, it looks for the generation that has the minimum error. Eventually, it optimizes the parameters of the generation with the minimum possible error. The response of the genetic algorithm with the best efficiency and the mean efficiency of sodium removal in different generations are presented in Figure 9. As can be seen, when generations increase, the conformity of these two figures increases as well, so that in the generation =135, the best and the mean efficiencies are matched and there will be no mutation or sudden change on it. Figure 9 is plotted to ensure more reliability of the first stage which is to find the most accurate generation. Here, the distances between all individual generations are presented. As it was expected, when the number of generations increases, the mean distance between them decreases, and in generation=135, this distance is almost zero. After determining the best generation, the optimum effective factors were determined in the sodium adsorption process. According to Figure 9, the optimum values of pH, contact time, adsorbent dosage, and Na^+ ion concentration were obtained 10.918, 46.967 min, 3.516 g/L, and 939.921 mg/L, respectively. Then, to check the accuracy of the genetic algorithm in the optimization of the conditions, all the results obtained in the laboratory (real conditions) were repeated and similar results were obtained. In the optimum conditions, the removal efficiency of Na^+ ion was obtained 94.23% by the genetic algorithm.

3. 6. Adsorption Isotherms

Adsorption isotherms are used to describe the equilibrium relationship between adsorbent and adsorbate in an aqueous solution. Also, they are the main factors in the design of sorption systems.[36] The most common isotherms are Freundlich and Langmuir isotherms. The Freundlich equilibrium isotherm is based on the multilayer and heterogeneous adsorption on the adsorbent. The linear form of this equation is expressed below:[37]

$$\ln q_e = \ln k_F + \frac{1}{n} \ln C_e \quad (4)$$

where, k_F (mg/g(L/mg)$^{1/n}$) and n are the Freundlich constants:[38]

The Langmuir isotherm model assumes monolayer sorption on a surface containing a limited number of uniform energy adsorption sites.[36] This model also states that adsorption only occurs on homogeneous sites, without any action between the adsorbate and adsorbent molecules.[39] The linear form of the Langmuir model is expressed as follows:

$$\frac{C_e}{q_e} = \frac{C_e}{q_o} + \frac{1}{k_L q_o} \quad (5)$$

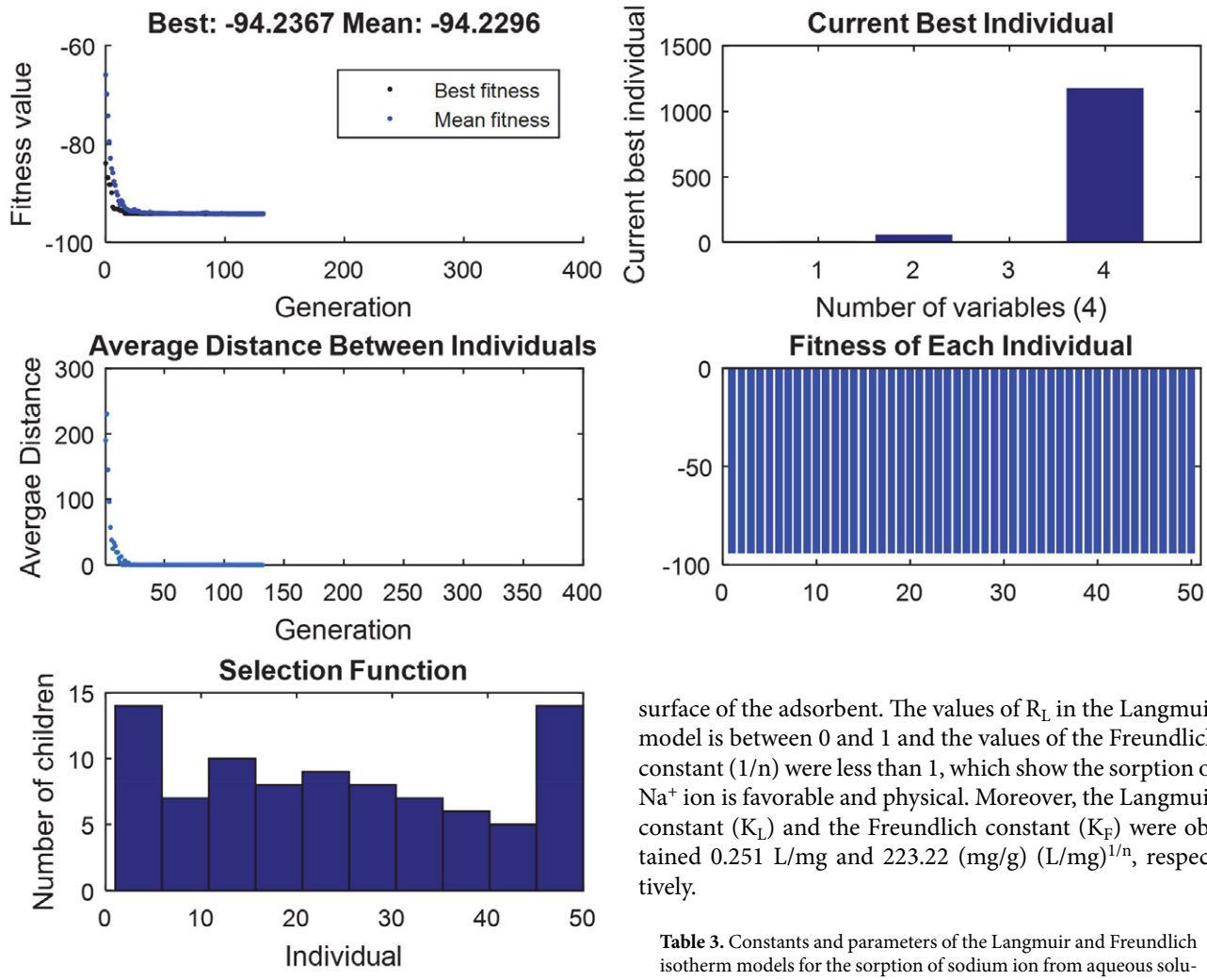

Figure 9. The optimization steps of adsorption parameters using genetic algorithm

where, k_L is the Langmuir constant (L/mg) and q_o is the maximum adsorbed amount per gram of the adsorbent (mg/g), C_e is the equilibrium concentration of the adsorbate (mg/L), and q_e is the initial amount of adsorbate at equilibrium (mg/g).

The value of the parameters of Langmuir and Freundlich models are presented in Table 3. Also, the plots of the Langmuir and Freundlich models for the sodium sorption process are shown in Figure 10. Considering the results, the maximum uptake capacity by the Langmuir model was determined 249.67 mg/g, which was a significant value. Also, the correlation coefficient for the Langmuir model (R^2 = 1) was greater than the Freundlich model (R^2 = 0.993). Therefore, in all three studied temperatures, the Langmuir model could better describe the equilibrium behavior of the sorption process, and the sorption process of sodium ion took place as monolayer on the homogeneous surface of the adsorbent. The values of R_L in the Langmuir model is between 0 and 1 and the values of the Freundlich constant (1/n) were less than 1, which show the sorption of Na^+ ion is favorable and physical. Moreover, the Langmuir constant (K_L) and the Freundlich constant (K_F) were obtained 0.251 L/mg and 223.22 (mg/g) $(L/mg)^{1/n}$, respectively.

Table 3. Constants and parameters of the Langmuir and Freundlich isotherm models for the sorption of sodium ion from aqueous solution using activated carbon

Isotherm	parameter	value
	q_0 (mg/g)	249.67
Langmuir	K_L(L/mg)	0.251
	R^2	1
Freundlich	K_F (mg/g)$(L/mg)^{1/n}$	223.22
	n	59.95
	R^2	0.993

3. 7. Adsorption Process Kinetics

It is necessary to study the process kinetics for the investigation of the effective parameters on the sorption rate. The sorption process may occur in several stages with different rates. Here, we just discuss the two main and common kinetic models that are quasi-first-order (QFO) and quasi-second-order (QSO) kinetic models.[19]

The QFO kinetic model is based on the sorption capacity in adsorption of a pollutant and is used when the

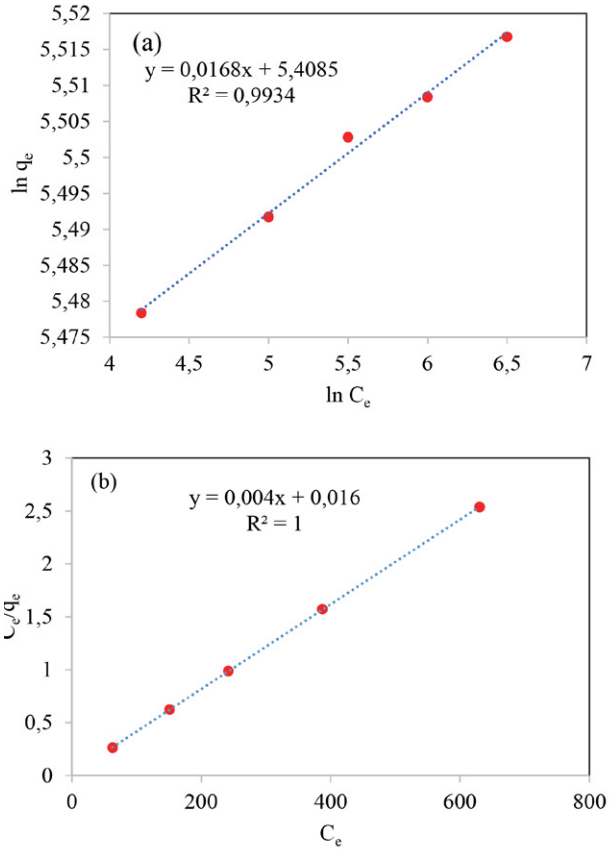

Figure 10. The Freundlich (a) and Langmuir (b) equilibrium isotherms

adsorption follows the diffusion mechanism through a boundary layer. The QFO model is described as follows:[17]

$$ln(q_e - q_t) = lnq_e - k_1 t \quad (6)$$

Where, q_e and q_t are the uptake capacity at equilibrium and at time t in terms of mg/g and k_1 is the QFO kinetic constant (min^{-1}).

Also, the linear form of the QSO kinetic model is define below:[17]

$$\frac{t}{q_t} = \frac{1}{k_2 q_e^2} + \frac{1}{q_e} t \quad (7)$$

The values obtained from the kinetic parameters of sodium adsorption on *Moringa oleifera*-derived AC are listed in Table 4. The results of kinetic models are also displayed in Figure 11. It can be seen that the correlation coefficient (R^2) for the QSO kinetic model is higher than the QFO kinetic model and is around 1, therefore sodium sorption by the AC follows the QSO kinetic model. Furthermore, the calculated values of uptake capacity ($q_{e\ cal}$) follows the QSO kinetic model.[17] Therefore, the QSO kinetic model was better fitted with the experimental data. Also, the constant values of the QFO and QSO models were determined 0.128 L/mg and 0.000463 L/mg, respectively.

Table 4. Constants and parameters of the QFO and QSO kinetic models for the sorption of sodium ion from aqueous solution using activated carbon

model	parameter	value
QFO	$q_{e,cal}$ (mg/g)	559.6
	K_1 (L/mg)	0.128
	R^2	0.8797
QSO	$q_{e,cal}$ (mg/g)	286.98
	K_2 (L/mg)	0.000463
	R^2	0.9959

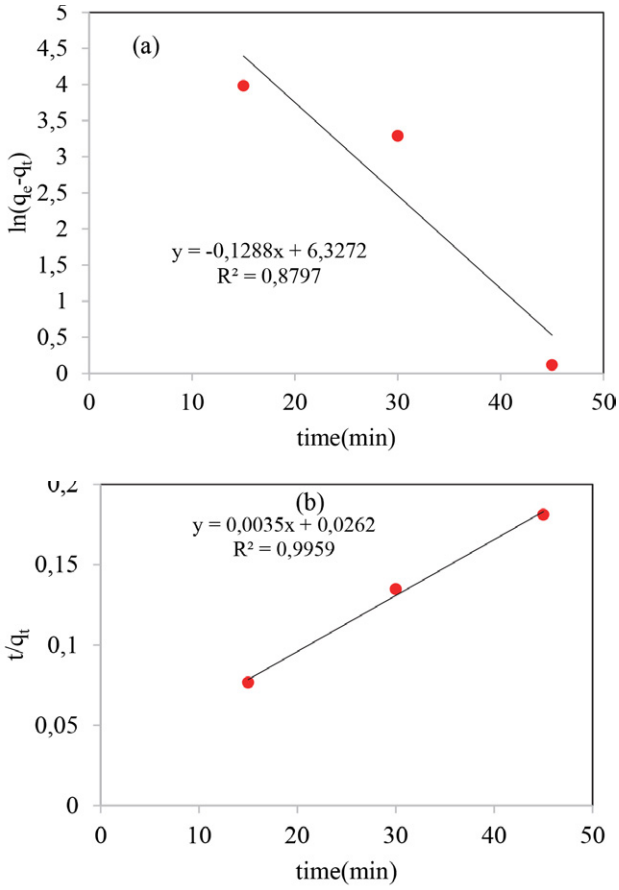

Figure 11. QFO (a) and QSO (b) kinetic models

3. 8. Thermodynamic Study

The thermodynamic parameters provide information about the spontaneity of the sorption process and an increase or decrease of randomness at the interface of solid-liquid. Also, they determine whether a sorption process is exothermic or endothermic.[40,41] Three main thermodynamic parameters should be determined to study the thermodynamics of the uptake process. These three parameters are changes of enthalpy (ΔH°), Gibbs free energy (ΔG°), and entropy (ΔS°). The values of ΔH° and ΔS° are obtained from the slope and intercept of the following equation:[42,43]

$$lnk_c = \frac{\Delta S^o}{R} - \frac{\Delta H^o}{RT} \quad (8)$$

$$K_c = \frac{q_e}{C_e} \quad (9)$$

Where, R is the global gas constant (8.314 J/mol K) and K_c (L/g) is the ratio of the adsorbed material on the adsorbate (mg/g) to the residual material in the solution (mg/L). The values of ΔG° is calculated from the following equation:

$$\Delta G^o = -RTlnK_c \quad (10)$$

Generally, the negative values of ΔG° show that the sorption process is spontaneous. The negative values of ΔH° show that the sorption process is exothermic and also it is favorable at lower temperatures.

The negative values of ΔS° indicate that the efficiency decreases as the temperature increases at the solid-liquid interface during the sorption process and it is vice versa for positive values.[44,45]

The values of thermodynamic parameters for the sodium ion adsorption using the AC are presented in Table 5. The experiments were done in the initial sodium concentration of 100 mg/L and temperatures of 20–50 °C. It is observed in Table 5 that the values of ΔH° and ΔS° are both negative and are –147 and –0.455 (kJ/mol), respectively. Also, the values of ΔG° for temperatures of 20, 35, and 50 °C are –16.208, –4.849, and –2.67 (kJ/mol), respectively. Moreover, the study of the thermodynamic parameters for the sodium ion adsorption using the AC showed that ΔH° had a negative value, which shows the Na^+ uptake process is exothermic, it also implies that the uptake process is more favorable in lower temperatures. Furthermore, the negative value of ΔS° is an indication of the reduction in efficiency and degree of freedom at the solid-liquid interface during the uptake process. Besides, the negative values of ΔG° indicate that the Na^+ uptake process is spontaneous.[39]

Table 5. Thermodynamic parameters for the sorption process of sodium ion from aqueous solution using activated carbon

Temperature (°C)	–ΔG° (kJ/mol)	ΔH°) (kJ/mol	ΔS° (kJ/mol K)
293	–16.208	–147	–0.455
308	–4.849		
323	–2.67		

3. 9. Final Comparison of the Adsorbents

After determining the optimal conditions for the removal of Na^+ from aqueous solution using AC, a comparison was done between AC and other adsorbents such as eggshell derived CaO and CaO/Fe_3O_4 composite and the results are shown in Figure 12. The experiments were done under optimal conditions such as pH of 11, contact time of 45 min, adsorbent dosage of 5 g/L, temperature of 25 °C and sodium ion concentration of 900 mg/L. As shown, the removal efficiency of Na^+ using AC (95.91%) is higher than CaO (83.45%) and CaO/Fe_3O_4 (89.2%), indicating the high performance of AC compared to the other two adsorbents.

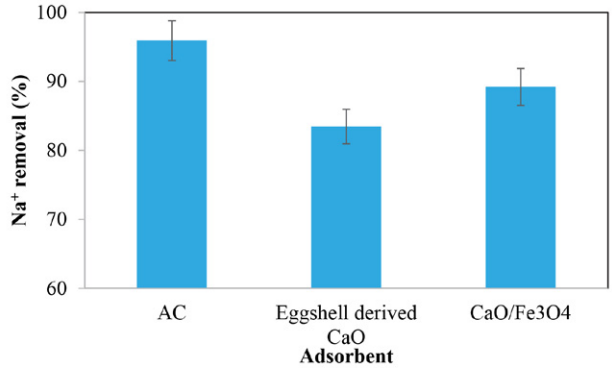

Figure 12. The removal efficiency of the adsorbents at optimal conditions (pH=11, time= 45 min, adsorbent dosage= 5 g/L, temperature =25 °C and initial sodium concentration= 900 mg/L)

4. Conclusion

The obtained results indicated that the AC made from *Moringa oleifera* plant is an effective adsorbent for the removal of sodium ion from aqueous solutions. Based on the present study, removal of sodium ion increases with increasing contact time and pH at room temperature however, it has an opposite relationship with the enhancement of sodium ion concentration. Furthermore, the studies indicated that the maximum sodium ion removal efficiency of 95.91% was achieved at contact time of 45 min, adsorbent dosage of 5 g/L, and pH of 11. Also, the equilibrium and kinetic studies indicated that the equilibrium data were better explained by the Langmuir isotherm than the Freundlich isotherm and the best kinetic correlation for sodium adsorption by the adsorbent in laboratory conditions follows the QSO kinetic model. Furthermore, the thermodynamic behavior of the Na^+ ion process indicated that the sodium ion sorption by the AC is spontaneous, exothermic, and possible. Moreover, the maximum uptake capacity of Na^+ ion was obtained 249.67 mg/g, which was a significant amount. Generally, *Moringa oleifera* can be used as an effective adsorbent for the removal of Na^+ ion from water and wastewater due to its benefits such as cheapness, nativity, and availability.

Disclosure statement

No potential conflict of interest was reported by the authors.

5. Reference

1. L. He, M. X. Li, F. Chen, S.S. Yang, J. Ding, L. Ding, N.Q. Ren, *J. Hazard. Mater*. **2021**, *417*, 126113. **DOI:**10.1016/j.jhazmat.2021.126113
2. S. Yang, Z. Li, K. Yan, X. Zhang, Z. Xu, W. Liu, Z. Liu, H. Liu, *J. Environ. Sci*. **2021**, *103*, 59–68. **DOI:**10.1016/j.jes.2020.10.013
3. M. Fathy, M. A. Mousa, T. A. Moghny, A. E. Awadallah, *Appl. Water Sci*. **2017**, *7*, 4427–4435. **DOI:**10.1007/s13201-017-0588-3
4. A. M. Siemens, J. J. Dynes, W. Chang, *Environ. Technol*. **2020**. **DOI**: 0.1080/09593330.2020.1721567
5. L. He, Y. Chen, J. Li, *Resour. Conserv. Recycl*., **2018**, *133*, 206–228. **DOI:**10.1016/j.resconrec.2018.02.015
6. K. C. Khulbe, T. Matsuura, *Appl. Water Sci*. **2018**, *8*, 19. **DOI:**10.1007/s13201-018-0661-6
7. Q. Guan, G. Zeng, J. Song, C. Liu, Z. Wang, S. Wu, *J. Environ. Manage.* **2021**, *293*, 112961. **DOI:**10.1016/j.jenvman.2021.112961
8. J. S. George, A. Ramos, H. J. Shipley, *J. Environ. Chem. Eng.* **2015**, *3*, 969–976. **DOI:**10.1016/j.jece.2015.03.011
9. S. Ren, B. Ye, S. Li, L. Pang, Y. Pan, H. Tang, *Nano Res*. **2021**. **DOI:**10.1007/s12274-021-3694-3
10. A. Garg, M. Mainrai, V. K. Bulasara, S. Barman, *Chem. Eng. Commun*. **2015**, *202*, 123–130. **DOI:**10.1080/00986445.2013.836636
11. T. Jesionowski, J. Zdarta, B. Krajewska, *Adsorption*, **2014**, *20*, 801–821. **DOI:**10.1007/s10450-014-9623-y
12. X. Cheng, L. He, H. Lu, Y. Chen, L. Ren, *J. Hydrol.*, **2016**, *540*, 412–422. **DOI:**10.1016/j.jhydrol.2016.06.041
13. S. Abbasi, R. Foroutan, H. Esmaeili, F. Esmaeilzadeh, *Desalin. Water Treat*. **2019**, *141*, 269. **DOI:**10.5004/dwt.2019.23569
14. R. Salahshour, M. Shanbedi, H. Esmaeili, *Acta Chim. Slov*. **2021**, *68*, 363–373. **DOI:**10.17344/acsi.2020.6311
15. A. R. Lucaci, D. Bulgariu, I. Ahmad, G. Lisă, A. M. Mocanu, L. Bulgariu, *Water*, **2019**, *11*, 1565. **DOI:**10.3390/w11081565
16. A. Attarad, Z. Hira, Z. Muhammad, H. Ihsanul, P. Abdul Rehman, S. Joham, H. Altaf, *Nanotechnol. Sci. Appl*. **2016**, *9*, 49–67. **DOI:**10.2147/NSA.S99986
17. S. M. Mousavi, S. A. Hashemi, H. Esmaeili, A. M. Amani, F. Mojoudi, *Acta Chim. Slov.* **2018**, *65*, 750–756. **DOI:**10.17344/acsi.2018.4536
18. A. A. Alqadami, M. Naushad, Z. A. Alothman, M. Alsuhybani, M. Algamdi, *J. Hazard. Mater*. **2020**, *389*, 121896. **DOI:**10.1016/j.jhazmat.2019.121896
19. R. Foroutan, R. Mohammadi, S. Farjadfard, H. Esmaeili, B. Ramavandi, G.A. Sorial, *Adv. Powder Technol*. **2019**, *30*, 2188–2199. **DOI:**10.1016/j.apt.2019.06.034
20. S. M. Jamil, M. W., Ali, A. Ripin, A. Ahmad, *J. Appl. Sci*. **2015**, *15*, 516–523. **DOI:**10.3923/jas.2015.516.523
21. R. Rostamian, M. Heidarpour, S. F. Mousavi, M. Afyuni, *J. Agr. Sci. Tech*. **2018**, *17*, 1057–1069.
22. R. Caletka, C. Konečný, M. Šimková, *J. Radioanal. Chem*. **1972**, *10*, 5–15. **DOI:**10.1007/BF02518760
23. S. Yang, X. Wan, K. Wei, W. Ma, Z. Wang, *Miner. Eng.* **2021**, *169*, 106966. **DOI:**10.1016/j.mineng.2021.106966
24. Z. Wang, Q. Lei, Z. Wang, H. Yuan, L. Cao, N. Qin, Z. Lu, J. Xiao, J. Liu, *Chem. Eng. J*. **2020**, *395*, 125180. **DOI:**10.1016/j.cej.2020.125180
25. K. Zhang, L. Qiu, J. Tao, X. Zhong, Z. Lin, R. Wang, Z. Liu, *Hydrometallurgy* **2021**, *205*, 105722. **DOI:**10.1016/j.hydromet.2021.105722
26. Z. Fan, P. P. Ji, J. Zhang, D. Segets, D. R. Chen, S. C. Chen, *J. Membr. Sci*. **2021**, *635*, 119503. **DOI:**10.1016/j.memsci.2021.119503
27. Q. Pan, Y. Zheng, Z. Tong, L. Shi, Y. Tang, *Angew. Chem. Int. Ed*. **2021**, *60*, 11835–11840. **DOI:**10.1002/anie.202103052
28. R. Chen, Y. Cheng, P. Wang, Y. Wang, Q. Wang, Z. Yang, C. Tang, S. Xiang, S. Luo, S. Huang, C. Su, *Chem. Eng. J.* **2021**, *421*, 129682. **DOI:**10.1016/j.cej.2021.129682
29. X. Li, T. Shi, B. Li, X. Chen, C. Zhang, Z. Guo, Q. Zhang, *Mater. Des*. **2019**, *183*, 108152. **DOI:**10.1016/j.matdes.2019.108152
30. R. Wang, Y. Yuan, J. Zhang, X. Zhong, J. Liu, Y. Xie, S. Zhong, Z. Xu, *J. Power Sources* **2021**, *501*, 230006. **DOI:**10.1016/j.jpowsour.2021.230006
31. S. Yang, X. Wan, K. Wei, W. Ma, Z. Wang, *Waste Manage*. **2021**, *120*, 820–827. **DOI:**10.1016/j.wasman.2020.11.005
32. R. Chen, Y. Cheng, P. Wang, Q. Wang, S. Wan, S. Huang, R. Su, Y. Song, Y. Wang, *Sci. Total Environ.* **2021**, *756*, 143871. **DOI:**10.1016/j.scitotenv.2020.143871
33. H. Yin, C. Han, Q. Liu, F. Wu, F. Zhang, Y. Tang, *Small* **2021**, *17*, 2006627. **DOI:**10.1002/smll.202006627
34. R. Foroutan, R. Mohammadi, H. Esmaeili, F.M. Bektashi, S. Tamjidi, Waste Manage. **2020**, *105*, 373–383. **DOI:**10.1016/j.wasman.2020.02.032
35. H. Li, B. Xu, G. Lu, C. Du, N. Huang, *Energy Convers. Manag.* **2021**, *236*, 114063. **DOI:**10.1016/j.enconman.2021.114063
36. G. Abbas, I. Javed, M. Iqbal, R. Haider, F. Hussain, N. Qureshi, *Desalin. Water Treat*. **2017**, *95*, 274–285. **DOI:**10.5004/dwt.2017.21465
37. I. Khoshkerdar, H. Esmaeili, *Acta Chim. Slov*. **2019**, *66*, 208–216. **DOI:**10.17344/acsi.2018.4795
38. L. P. Lingamdinne, J. S. Choi, J. K. Yang, Y. Y. Chang, J. R. Koduru, J. Singh, *Acta Chim. Slov*. **2018**, *65*, 599–610. **DOI:**10.17344/acsi.2018.4254
39. D. Humelnicu, M. Ignat, M. Suchea, *Acta Chim. Slov*. **2015**, *62*, 947–957. **2016**, *107*, 012067. **DOI:**10.17344/acsi.2014.1825
40. W. Y. Huang, G. Q. Wang, W. H. Li, T. T. Li, G. J. Ji, S. C. Ren, M. Jiang, L. Yan, H. T. Tang, Y. M. Pan, Y. J. Ding, *Chem* **2020**, *6*, 2300–2313. **DOI:**10.1016/j.chempr.2020.06.020
41. A. Awwad, M. Amer, M. Al-aqarbeh, *Chem. Int. 2020*.
42. W. Y. Huang, D. Li, Z. Q. Liu, Q. Tao, Y. Zhu, J. Yang, Y. M. Zhang, *Chem. Eng. J*. **2014**, *236*, 191–201. **DOI:**10.1016/j.cej.2013.09.077
43. F. Takmil, H. Esmaeili, S.M. Mousavi, S.A. Hashemi, *Adv. Powder Technol*. **2020**, *31*, 3236–3245. **DOI:**10.1016/j.apt.2020.06.015
44. J. Fu, Z. Chen, M. Wang, S. Liu, J. Zhang, J. Zhang, Q. Xu, *Chem. Eng. J*. **2015**, *259*, 53–61. **DOI:**10.1016/j.cej.2014.07.101
45. Z. Li, M. Peng, X. Zhou, K. Shin, S. Tunmee, X. Zhang, C. Xie, H. Saitoh, Y. Zheng, Z. Zhou, Y. Tang, *Adv. Mater.* **2021**, 2100793. **DOI:**10.1002/adma.202100793

Povzetek

Namen študije je bil določiti optimalni adsorbent izmed aktivnega oglja na osnovi *Moringa oleifera* (AC), CaO nanodelcev pridobljenih in jajčnih lupin in CaO/Fe_3O_4 za odstranjevanje natrijevih (Na^+) ionov iz vodnih raztopin. V prvem koraku smo določili njihovo adsorpcijsko učinkovitost, pri čemer se je AC adsorbent izkazal kot najboljši. Z *metodologijo* odzivnih *ploskev* (ang. response surface methodology – RSM) smo ovrednotili vpliv različnih parametrov na učinkovitost adsorpcije (Na^+) ionov AC adsorbenta. Najvišja učinkovitost odstranjevanja pod optimalnimi pogoji je znašala 95.91 %, pri pH vrednosti 11, kontaktnem času 45 min, temperaturi 25 °C, koncentraciji natrijevih ionov 900 mg/L in količini adsorbenta 5 g/L. Optimalni pogoji določeni z uporabo genetskih algoritmov pa so bili pri kontaktnem času 94.97 min, količini adsorbenta 3.52 g/L, koncentraciji natrijevih ionov 939.92 mg/L in pH vrednosti 10.92. Maksimalna adsorpcijska kapaciteta določena z Langmuirjevim modelom je bila ocenjena na 249.67 mg/g, kar je znatna količina. Poleg tega smo pokazali, da lahko eksperimentalne podatke ravnotežja in kinetike adsorpcije natrijevih ionov dobro opišemo z Langmuirjevo izotermo in kinetiko adsorpcije psevdo-drugega-reda. Termodinamična analiza je pokazala, da je adsorpcija endotermen proces. Zaključimo lahko, da je predstavlja aktivno oglje, z visoko učinkovitostjo odstranjevanja in visoko adsorpcijsko kapaciteto, obetajoč adsorbent za odstranjevanje natrija iz onesnaženih voda na industrijskem nivoju.